

## TCG-S: Orthogonal Coupling of P\*-Admissible Representations for General Floorplans

Jai-Ming Lin and Yao-Wen Chang

**Abstract**—In this paper, we extend the concept of the P-admissible floorplan representation to that of the P\*-admissible one. A P\*-admissible representation can model the most general floorplans. Each of the currently existing P\*-admissible representations, sequence pair (SP), bounded-slicing grid, and transitive closure graph (TCG), has its strengths as well as weaknesses. We show the equivalence of the two most promising P\*-admissible representations, TCG and SP, and integrate TCG with a packing sequence (part of SP) into a representation, called TCG-S. TCG-S combines the advantages of SP and TCG and at the same time eliminates their disadvantages. With the property of SP, a fast packing scheme is possible. Inherited nice properties from TCG, the geometric relations among modules are transparent to TCG-S (implying faster convergence to a desired solution), placement with position constraints becomes much easier, and incremental update for cost evaluation can be realized. These nice properties make TCG-S a superior representation which exhibits an elegant solution structure to facilitate the search for a desired floorplan/placement. Extensive experiments show that TCG-S results in the best area utilization, wirelength optimization, convergence speed, and stability among existing works and is very flexible in handling placement with special constraints.

**Index Terms**—Floorplanning, layout, physical design, transitive closure graph.

### I. INTRODUCTION

As technology advances, the circuit size in modern very large scale integration (VLSI) design increases dramatically. To handle the increasing design complexity, hierarchical designs and IP modules are widely used to optimize area and timing for design convergence. Further, the need to integrate heterogeneous systems or special modules imposes some placement constraints, e.g., the boundary-module constraint which requires some modules to be placed along the chip boundaries for shorter connections to pads, the preplaced-module constraint which preassigns modules to specific positions, etc. These trends make floorplanning/placement much more important than ever, and it is of particular significance to consider the floorplanning/placement with various constraints. To cope with these challenges, it is desired to develop an efficient and effective floorplan representation that can model the geometric relations among regular as well as constrained modules.

Many floorplan representations have been proposed in the literature, e.g., slicing tree [16], normalized Polish expression [19], sequence pair (SP) [13], bounded-slicing grid (BSG) [15], O-tree [3], B\*-tree [1], corner block list (CBL) [4], and transitive closure graph (TCG) [9]. Unlike the traditional classification of the slicing and nonslicing structures, we can alternatively classify them into two categories, P\*-admissible and non-P\*-admissible representations. A representation is said to be P-admissible if it satisfies the following four conditions [13]: 1) the solution space is finite; 2) every solution is feasible; 3) packing and cost evaluation can be performed in polynomial time;

and 4) the best evaluated packing in the space corresponds to an optimal placement. We extend in this paper the concept of the P-admissible representation to that of the P\*-admissible one by adding the fifth condition: 5) both horizontal and vertical [and thus two dimensional (2-D)] geometrical information between modules are defined in the representation. With this condition, any placement can be modeled. Therefore, a P\*-admissible representation can represent the most general floorplans and contains a complete structure for searching for an optimal floorplan/placement solution. It is thus desirable to develop an effective and flexible P\*-admissible representation.

Among the existing popular representations, SP, BSG, and TCG are P\*-admissible while slicing tree, normalized Polish expression (NPE), O-tree, B\*-tree, and CBL are not. The slicing tree and normalized Polish expression are intended for slicing floorplans only. Since an optimal placement could be a nonslicing structure, the two representations are not P\*-admissible [i.e., violation of P\*-admissible Condition (4)]. An O-tree defines only one-dimensional geometrical relation between compacted modules and thus can obtain the relation in the other dimension only after packing [i.e., violation of Condition (5)]. [Note that O-tree is undefined for some uncompact placements which may correspond to the best solutions for wirelength optimization. Therefore, as far as wirelength optimization is concerned, O-tree is not even P-admissible since Condition (4) is violated.] A B\*-tree requires a placement to be left and/or bottom compacted. If the placement after a tree packing is not compacted, a sequence of compaction operations are applied to make all modules compacted to the left and/or bottom. However, the space intended for placing a module may be occupied by previously placed modules during packing, resulting in a mismatch between the original representation and its compacted placement. Therefore, it may not be feasible to find a compacted placement corresponding to the original B\*-tree, and thus it is not P\*-admissible [i.e., violation of Condition (2)]. CBL can represent only mosaic floorplans, in which each region in the floorplan contains exactly one module. CBL is not P\*-admissible because it cannot guarantee a feasible solution after a perturbation [i.e., violation of Condition (2)]. Non-P\*-admissible representations intrinsically have a smaller solution space and lower packing cost since their corresponding floorplanning/placement structures are more restricted [e.g., slicing structures (slicing tree, NPE), compacted placements (O-tree, B\*-tree), mosaic floorplans (CBL), etc.]. However, lack of the guarantee in the feasibility and/or the optimality of their representations would inevitably lead to longer running times and/or lower solution quality.

The existing P\*-admissible representations, SP, BSG, and TCG, have their own distinct properties as well as common ones. Nevertheless, researchers tend to favor SP over BSG because BSG incurs many redundancies and thus a much larger solution space, implying a longer running time to search for a good solution. Therefore, we shall focus on SP and TCG. Both SP and TCG are considered very flexible representations and construct constraint graphs to evaluate their packing cost. SP consists of two sequences of modules ( $\Gamma_+$ ,  $\Gamma_-$ ), where  $\Gamma_+$  specifies the module ordering from top-left to bottom-right and  $\Gamma_-$  from bottom-left to top-right. Hence,  $\Gamma_-$  corresponds to the ordering for packing modules to the bottom-left direction and thus can be used to guide module packing. However, like most existing representations (e.g., NPE, BSG, O-tree, B\*-tree, CBL) the geometric relations between modules are *not transparent* to the operations of SP (i.e., the effect of an operation on the change of module relation is not clear before packing) and, thus, we need to construct constraint graphs from scratch after each perturbation to evaluate the packing cost; this deficiency makes SP harder to converge to a desired solution and to handle placement with constraints (e.g., boundary modules, preplaced modules, etc.).

Manuscript received October 21, 2002; revised February 2, 2003 and May 18, 2003. This work was supported in part by the National Science Council of Taiwan R.O.C. under Grant No. NSC-89-2215-E-009-117. This paper was recommended by Associate Editor M. D. F. Wong.

J.-M. Lin is with the Department of Computer and Information Science, National Chiao Tung University, Hsinchu 300, Taiwan (e-mail: gis87808@cis.nctu.edu.tw).

Y.-W. Chang is with the Graduate Institute of Electronics Engineering & the Department of Electrical Engineering, National Taiwan University, Taipei 106, Taiwan (e-mail: ywchang@cc.ee.ntu.edu.tw).

Digital Object Identifier 10.1109/TCAD.2004.828114

TCG consists of a horizontal transitive closure graph  $C_h$  to define the horizontal geometric relations between modules and a vertical one  $C_v$  for vertical geometric relations. Contrast to SP, the geometric relations between modules are transparent to TCG as well as its operations, facilitating the convergence to a desired solution. Further, TCG supports incremental update during operations and keeps the information of boundary modules as well as the shapes and the relative positions of modules in the representation. Nevertheless, like SP, constraint graphs are also needed for TCG to evaluate its packing cost, and unlike SP, we need to perform extra operations to obtain the module packing sequence.

Therefore, an interesting question arises. Is it possible to develop a representation that can combine the advantages of SP and TCG and at the same time eliminate their disadvantages? We answer this question in affirmation by showing the equivalence of TCG and SP, and integrating them into TCG-S  $S = (C_h, C_v, \Gamma_-)$ . The orthogonal combination leads to a representation with at least the following advantages:

- With the property of SP, a fast  $O(m \lg m)$ -time packing scheme is possible for a  $P^*$ -admissible representation, where  $m$  is the number of modules. (Note that a linear-time packing scheme is possible for the tree-based representations, but they can represent only more restricted compacted floorplans.)
- It is clear later that the sequence  $\Gamma_-$  is the topological order of both  $C_h$  and  $C_v$  and is thus uniquely determined by  $C_h$  and  $C_v$ . Therefore, the combination will not incur any redundancy over the original TCG, and the solution space of TCG-S is still  $(m!)^2$  (same as TCG and SP), where  $m$  is the number of modules.
- Inherited from TCG, the geometric relations among modules are transparent to TCG-S, implying faster convergence to a desired solution.
- Inherited from TCG, placement with position constraints becomes much easier.
- Inherited from TCG, TCG-S can support incremental update for cost evaluation.

These nice properties make TCG-S an effective, efficient, and flexible representation. Extensive experiments based on a set of commonly used Microelectronics Center of North Carolina (MCNC) benchmarks show that TCG-S results in the best area utilization, wirelength optimization, convergence speed, and solution stability among existing works. (Note that we also consider the convergence speed and stability to eliminate the possible unfairness due to the nondeterministic behavior of simulated annealing, which were neglected in most previous works.)

To show the flexibility of TCG-S, we also consider placement with preplaced and boundary modules. For placement with preplaced modules, Murata *et al.* [14] proposed an *adaptation algorithm* to transform an infeasible SP with preplaced modules into a feasible one. However, the process incurs expensive computations. For placement with the boundary-module constraint, Tang and Wong in [18] handled the constraint by adding dummy edges into the constraint graphs of SP. Ma *et al.* in [12] assigned a penalty to a misplaced boundary module and perturbed the CBL to reduce the penalty. However, both [18] and [12] cannot guarantee a feasible solution in each perturbation and their final placements. Lai *et al.* in [7] gave the feasibility conditions for SP with boundary modules and transformed an infeasible solution into a feasible one. However, the method is very complex, and many rules are needed to cope with the constraints.

In this paper, we also present the methods for handling placement with preplaced and boundary modules. Different from the previous works on boundary modules that cannot guarantee a feasible solution or need to transform an infeasible solution into a feasible one, TCG-S can easily maintain the feasibility during each perturbation. We compared our work with [7] on placement with boundary modules. (Note that there are no common benchmark circuits for this constraint.)

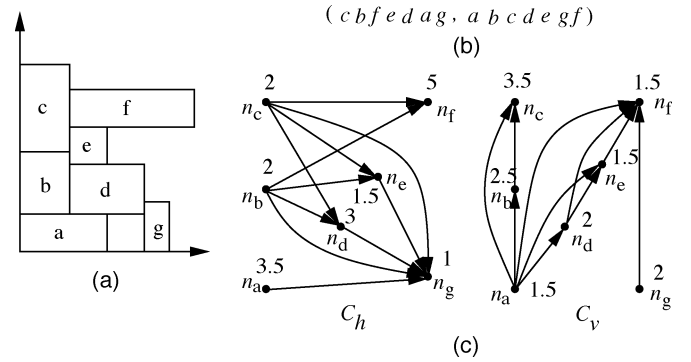


Fig. 1. (a) A placement. (b) The corresponding SP of (a). (c) The corresponding TCG of (b).

Experimental results show that TCG-S results in smaller areas than [7].

The remainder of this paper is organized as follows. Section II formulates the floorplan/placement design problem. Section III compares SP and TCG. Section IV presents the procedures to build the TCG-S from a placement and construct the placement from a TCG-S. Section V gives the operations to perturb a TCG-S. Section VI presents our methods to handle placement with boundary and preplaced modules. Experimental results are reported in Section VII. Finally, we give concluding remarks in Section VIII.

## II. PROBLEM DEFINITION

Let  $B = \{b_1, b_2, \dots, b_m\}$  be a set of  $m$  rectangular modules whose width, height, and area are denoted by  $W_i$ ,  $H_i$ , and  $A_i$ ,  $1 \leq i \leq m$ . Let  $(x_i, y_i)$  ( $(x'_i, y'_i)$ ) denote coordinate of the bottom-left (top-right) corner of module  $b_i$ ,  $1 \leq i \leq m$ , on a chip. A placement  $\mathcal{P}$  is an assignment of  $(x_i, y_i)$  for each  $b_i$ ,  $1 \leq i \leq m$ , such that no two modules overlap. The goal of floorplanning/placement is to optimize the area (i.e., the minimum bounding rectangle of  $\mathcal{P}$ ) and/or the wirelength (i.e., the summation of half bounding box of interconnections) induced by the assignment of  $b_i$ 's on the chip.

## III. $P^*$ -ADMISSIBLE REPRESENTATIONS

In this section, we first review the two  $P^*$ -admissible representations, TCG and SP, then show their equivalence, and compare their properties.

### A. Review of TCG and SP

TCG describes the geometric relations between modules based on two graphs, namely a *horizontal transitive closure graph*  $C_h$  and a *vertical transitive closure graph*  $C_v$ , in which a node  $n_i$  represents a module  $b_i$  and an edge  $(n_i, n_j)$  in  $C_h$  ( $C_v$ ) denotes that module  $b_i$  is left to (below) module  $b_j$ . TCG has the following three *feasibility properties* [9]:

- 1)  $C_h$  and  $C_v$  are acyclic.
- 2) Each pair of nodes must be connected by exactly one edge either in  $C_h$  or in  $C_v$ .
- 3) The transitive closure of  $C_h$  ( $C_v$ ) is equal to  $C_h$  ( $C_v$ ) itself.<sup>1</sup>

Fig. 1(a) shows a placement with seven modules  $a, b, c, d, e, f$ , and  $g$  whose widths and heights are (3.5, 1.5), (2, 2.5), (2, 3.5), (3, 2), (1.5, 1.5), (5, 1.5), and (1, 2), respectively. Fig. 1(c) shows the TCG  $= (C_h, C_v)$  corresponding to the placement of Fig. 1(a). The

<sup>1</sup>The transitive closure of a directed acyclic graph  $G$  is defined as the graph  $G' = (V, E')$ , where  $E' = \{(n_i, n_j) : \text{there is a path from node } n_i \text{ to node } n_j \text{ in } G\}$ .

value associated with a node in  $C_h$  ( $C_v$ ) gives the width (height) of the corresponding module, and the edge  $(n_i, n_j)$  in  $C_h$  ( $C_v$ ) denotes the horizontal (vertical) relation of  $b_i$  and  $b_j$ . Since there exists an edge  $(n_a, n_g)$  in  $C_h$ , module  $b_a$  is left to  $b_g$ . Similarly,  $b_a$  is below  $b_b$  since there exists an edge  $(n_a, n_b)$  in  $C_v$ .

SP uses a pair of sequences  $(\Gamma_+, \Gamma_-)$  to represent a floorplan/placement, where  $\Gamma_+$  and  $\Gamma_-$  give two permutations of module names. The geometric relation of modules can be derived from an SP as follows. Module  $b_a$  is left (right) to module  $b_b$  if  $a$  appears before (after)  $b$  in both  $\Gamma_+$  and  $\Gamma_-$ . Module  $b_a$  is below (above) module  $b_b$  if  $b$  appears before (after)  $a$  in  $\Gamma_+$  and  $a$  appears before (after)  $b$  in  $\Gamma_-$ . Fig. 1(b) shows the corresponding SP. Since  $a$  is before  $g$  in both  $\Gamma_+$  and  $\Gamma_-$ , module  $b_a$  is left to module  $b_g$ . Similarly,  $b_a$  is below  $b_b$  since  $a$  is after  $b$  in  $\Gamma_+$  and before  $b$  in  $\Gamma_-$ .

It is an important observation that the sequence  $\Gamma_-$  is the topological order of both  $C_h$  and  $C_v$  and is thus uniquely determined by  $C_h$  and  $C_v$ . For example, as shown in Fig. 1(b) and (c),  $\Gamma_- = \langle abcdefg \rangle$  is the topological order of both  $C_h$  and  $C_v$ . The observation is the key to the nonredundant combination of TCG and SP, which is the theme of this paper.

### B. Equivalence of SP and TCG

Like the relations between a skewed slicing tree [16] and an NPE [19] for slicing floorplans as well as O-tree and B\*-tree for nonslicing floorplans, TCG and SP are equivalent.

We can transform between TCG and SP as follows: Let the *fanin* (*fanout*) of a node  $n_i$ , denoted by  $F_{in}(n_i)$  ( $F_{out}(n_i)$ ), be the nodes  $n_j$ 's with edges  $(n_j, n_i)$  ( $(n_i, n_j)$ ). Given a TCG, we can obtain a sequence  $\Gamma_+$  by repeatedly extracting a node  $n_i$  with  $F_{in}(n_i) = \emptyset$  in  $C_h$  and  $F_{out}(n_i) = \emptyset$  in  $C_v$ , and then deleting the edges  $(n_i, n_j)$ 's ( $(n_j, n_i)$ 's) from  $C_h$  ( $C_v$ ) until no node is left in  $C_h$  ( $C_v$ ). Similarly, we can transform a TCG into another sequence  $\Gamma_-$  by repeatedly extracting the node  $n_i$  with  $F_{in}(n_i) = \emptyset$  both in  $C_v$  and  $C_h$ , and then deleting the edges  $(n_i, n_j)$ 's from both  $C_h$  and  $C_v$  until no node is left in  $C_h$  and  $C_v$ . Given an SP  $(\Gamma_+, \Gamma_-)$ , we can obtain a unique TCG  $(C_h, C_v)$  from the two constraint graphs of the SP by removing the source, sink, and associated edges. For example, the SP of Fig. 1(b) is equivalent to the TCG of Fig. 1(c). It is proved in [9] that there exists a one-to-one correspondence between TCG and SP.

### C. Comparison Between TCG and SP

Although TCG and SP are equivalent, their properties and induced operations are significantly different. Both SP and TCG are considered very flexible representations and construct constraint graphs to evaluate their packing cost.  $\Gamma_-$  of an SP corresponds to the ordering for packing modules to the bottom-left direction and thus can be used for guiding module packing. However, like most existing representations, the geometric relations among modules are not transparent to the operations of SP (i.e., the effect of an operation on the change of module relation is not clear before packing), and thus we need to construct constraint graphs from scratch after each perturbation to evaluate the packing cost; this deficiency makes SP harder to converge to a desired solution and to handle placement with constraints (e.g., boundary modules, preplaced modules, etc).

Contrast to SP, the geometric relations among modules are transparent to TCG as well as its operations, facilitating the convergence to a desired solution. Further, TCG supports incremental update during operations and keeps the information of boundary modules as well as the shapes and the relative positions of modules in the representation. Unlike SP, nevertheless, we need to perform extra operations to obtain the module packing sequence and an additional  $O(m^2)$  time to find a special type of edges, called *reduction edges*, in  $C_h$  ( $C_v$ ) for some operations. (We will define the edges later.)

For both SP and TCG, the packing scheme by applying the longest path algorithm is time-consuming since all edges in the constraint graphs are processed, even though they are not on the longest path. As shown in  $C_h$  of Fig. 1(c), if we add a source with zero weight and connect it to those nodes with zero in-degree, the  $x$  coordinate of each module can be obtained by applying the longest path algorithm on the resulting directed acyclic graph. Therefore, we have  $x_g = \max\{x'_a, x'_b, x'_c, x'_d, x'_e\}$ . To reduce the number of modules considered for placing a module, we introduce the concept of a horizontal (vertical) contour, denoted by  $R_h$  ( $R_v$ ).  $R_h$  ( $R_v$ ) is a list of modules  $b_i$ 's for which there exists no module  $b_j$  with  $y_j \geq y'_i$  ( $x_j \geq x'_i$ ) and  $x'_j \geq x'_i$  ( $y'_j \geq y'_i$ ); that is,  $R_h$  ( $R_v$ ) is a list of modules in the horizontal (vertical) contour. For the placement of Fig. 1(a), for example,  $R_h = \langle b_c, b_f \rangle$  and  $R_v = \langle b_g, b_d, b_e, b_f, b_c \rangle$ . To place a new module, we only need to consider the bends (and thus the modules) in the contour, and thus the packing time can be improved.

Suppose we have packed the modules  $b_a, b_b, b_c, b_d$ , and  $b_e$  based on the sequence  $\Gamma_-$ . Then, the resulting horizontal contour  $R_h = \langle b_c, b_e, b_d \rangle$ . Keeping  $R_h$ , we only need to traverse the contour from  $b_e$ , the successor of  $b_e$  (in terms of in-order search tree traversal), to the last module  $b_d$ , which have a horizontal relation with  $b_g$  (since there is an edge  $(n_d, n_g)$  in  $C_h$ ). Thus, we have  $x_g = x'_d$ . Packing modules in this way, we only need to consider  $x_e$  and  $x_d$ , and can get rid of the computation for a maximum value, leading to a faster packing scheme. We will show later how to apply a balanced binary tree to implement the contour operation to get a loglinear-time packing scheme.

## IV. TCG-S REPRESENTATION

Combining TCG  $(C_h, C_v)$  and SP  $(\Gamma_+, \Gamma_-)$ , we develop a representation, called TCG-S  $(C_h, C_v, \Gamma_-)$ , which uses horizontal and vertical transitive closure graphs as well as the packing sequence  $\Gamma_-$  to represent a placement. With the characteristics of TCG and SP, TCG-S has the following four *feasibility properties*.

- 1)  $C_h$  and  $C_v$  are acyclic.
- 2) Each pair of nodes must be connected by exactly one edge either in  $C_h$  or in  $C_v$ .
- 3) The transitive closure of  $C_h$  ( $C_v$ ) is equal to  $C_h$  ( $C_v$ ) itself.
- 4) The packing sequence  $\Gamma_-$  is the topological order of both  $C_h$  and  $C_v$ .

In this section, we first introduce how to construct  $\Gamma_-$ ,  $C_h$ , and  $C_v$  from a placement. Then, we propose an  $O(m \lg m)$ -time packing scheme for TCG-S, where  $m$  is the number of modules.

### A. From a Placement to TCG-S

In this section, we first introduce the procedure to extract  $\Gamma_-$  from a placement, and then construct  $C_h$  and  $C_v$  according to  $\Gamma_-$ .

For two nonoverlapped modules  $b_i$  and  $b_j$ ,  $b_i$  is said to be *horizontally (vertically) related* to  $b_j$ , denoted by  $b_i \vdash b_j$  ( $b_i \perp b_j$ ), if  $b_i$  is left to (below)  $b_j$  and their projections on the  $y$  ( $x$ ) axis overlap. For two nonoverlapped modules  $b_i$  and  $b_j$ ,  $b_i$  is said to be *diagonally related* to  $b_j$  if  $b_i$  is left to  $b_j$  and their projections on the  $x$  and the  $y$  axes do not overlap. To simplify the operations on geometric relations, a diagonal relation for modules  $b_i$  and  $b_j$  is treated as a horizontal one unless there exists a chain of vertical relations from  $b_i$  ( $b_j$ ), followed by the modules overlapped with the rectangle defined by the two closest corners of  $b_i$  and  $b_j$ , and finally to  $b_j$  ( $b_i$ ), for which it is considered as  $b_i \perp b_j$  ( $b_j \perp b_i$ ).

Given a placement,  $\Gamma_-$  can be extracted as follows. We first extract the module on the bottom-left corner. At each iteration, we extract the left-most unvisited module  $b$  with all the modules below  $b$  having been

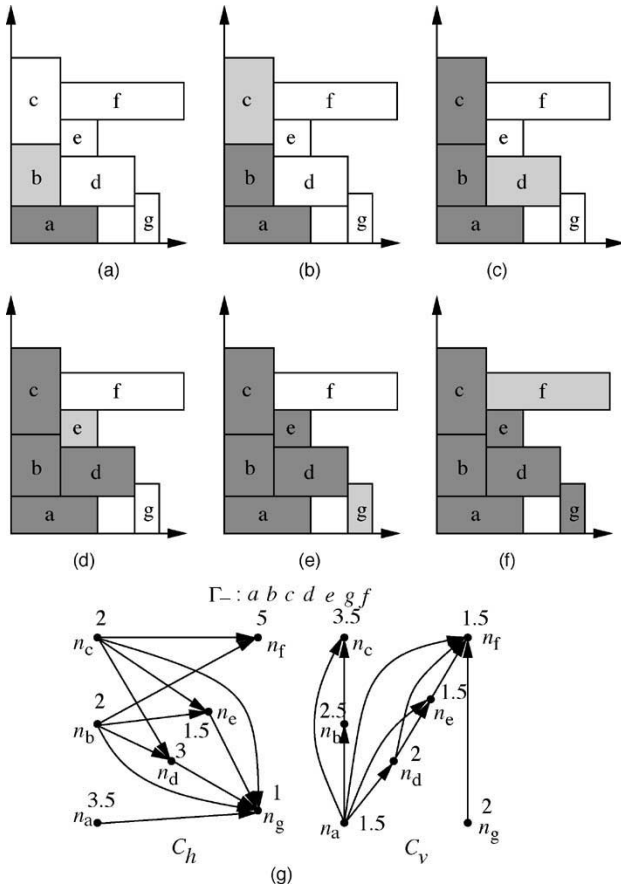


Fig. 2. (a)–(f) Process to extract a  $\Gamma_-$  from the placement of Fig. 1(a). (g) Resulting TCG-S.

extracted. The process repeats until no module left. Fig. 2(a)–(f) illustrate the procedure to extract a  $\Gamma_-$  from the placement of Fig. 1(a). We first extract the module  $b_a$  on the bottom-left corner [see Fig. 2(a)], and then  $b_b$  since it is the left-most module with all the modules below  $b_b$  having been extract [see Fig. 2(b)]. This process continues until no module is left, resulting in  $\Gamma_- = \langle abcdefg \rangle$ .

After extracting  $\Gamma_-$ , we can construct  $C_h$  and  $C_v$  based on  $\Gamma_-$ . For each module  $b_i$  in  $\Gamma_-$ , we introduce a node  $n_i$  with the weight being  $b_i$ 's width (height) in  $C_h$  ( $C_v$ ). Also, for each module  $b_i$  before  $b_j$  in  $\Gamma_-$ , we introduce an edge  $(n_i, n_j)$  in  $C_h$  ( $C_v$ ) if  $b_i \vdash b_j$  ( $b_i \perp b_j$ ). As shown in Fig. 2(b) and (g), for the first two modules  $b_a, b_b$  in  $\Gamma_-$ , we introduce the nodes  $n_a$  and  $n_b$  in  $C_h$  ( $C_v$ ) and assign the weights as their widths (heights). Also, we construct a directed edge  $(n_a, n_b)$  in  $C_v$  since module  $b_a$  is before  $b_b$  and  $b_a \perp b_b$ . The process repeats for all modules in  $\Gamma_-$ , resulting in the TCG-S shown in Fig. 2(g). Each transitive closure graph has seven nodes and 21 edges in total (eleven in  $C_h$  and ten in  $C_v$ ). We have the following theorem.

**Theorem 1:** There exists a unique TCG-S corresponding to a placement.

*Proof:* TCG-S is composed of three tuples  $C_h, C_v,$  and  $\Gamma_-$ . To get  $\Gamma_-$  from a placement, we repeatedly extract the left-most unvisited module  $b$  with all modules below  $b$  having been visited. The process repeats until all modules have been visited. Since such a module is unique in each iteration, the resulting  $\Gamma_-$  is unique. For each pair of modules  $b_i$  and  $b_j$  in  $\Gamma_-$ , say  $\langle \dots b_i \dots b_j \dots \rangle$ , there exists a unique relation ( $b_i \perp b_j$  or  $b_i \vdash b_j$ ) between the two modules in the placement based on the definition of TCG. Therefore, there exist unique  $C_h$  and  $C_v$  corresponding to the placement if we construct a node  $n_i$  (or an

edge  $(n_i, n_j)$ ) for each module  $b_i$  (or for each pair of modules  $b_i$  and  $b_j$  based on their geometric relation) in  $\Gamma_-$ .

To show that the 3-tuple  $C_h, C_v, \Gamma_-$  is a TCG-S, we prove that it satisfies the four TCG-S feasibility properties. Properties 1–3 are inherited from TCG. See the proof of Property 1 in [11]. For  $\Gamma_-$ , we repeatedly extract the left- and bottom-most unvisited module  $b$  until all modules have been processed. The left-most (bottom-most) module corresponds to the node in  $C_h$  ( $C_v$ ) with in-degree equal to zero. Therefore, the packing sequence  $\Gamma_-$  is the topological order of both  $C_h$  and  $C_v$ .<sup>2</sup> ■

## B. From TCG-S to a Placement

In this section, we propose an  $O(m \lg m)$ -time packing scheme based on  $\Gamma_-$  as well as a horizontal and a vertical contours  $R_h$  and  $R_v$ , where  $m$  is the number of modules. The basic idea is to process the modules based on the sequence defined in  $\Gamma_-$ , and then pack the current module to a corner formed by two previously placed modules in  $R_h$  ( $R_v$ ) according to the geometric relation defined in  $C_h$  ( $C_v$ ).

We detail the packing scheme as follows. Recall that the horizontal contour  $R_h$  (the vertical contour  $R_v$ ) is a list of modules  $b_i$ 's for which there exists no module  $b_j$  with  $y_j \geq y_i$  ( $x_j \geq x_i$ ) and  $x_j' \geq x_i'$  ( $y_j' \geq y_i'$ ). We can keep the modules  $b_i$ 's in  $R_h$  ( $R_v$ ) in a balanced binary search tree (e.g., the Red-Black tree [2])  $T_h$  ( $T_v$ ); the search-tree (in-order traversal) order in  $T_h$  ( $T_v$ ) corresponds to a nondecreasing order of the right (top) boundaries of the modules in the contour  $R_h$  ( $R_v$ ); i.e., the coordinates of the right (top) boundaries are sorted and kept as the search-tree order in the binary search tree  $T_h$  ( $T_v$ ). By ordering, in the following discussions, we refer to the search-tree order. (It is clear later that this important property leads to an efficient packing algorithm to be introduced shortly.) For easier presentation, we add a *dummy module*  $b_s$  ( $b_t$ ) to  $R_h$  ( $R_v$ ) to denote the left (bottom) boundary module of a placement. We have  $b_s \vdash b_i$  and  $b_t \perp b_i, \forall b_i$ . Let  $(x'_s, y'_s) = (0, \infty)$  and  $(x'_t, y'_t) = (\infty, 0)$ .  $R_h$  ( $R_v$ ) consists of  $b_s$  ( $b_t$ ) initially, as does the corresponding  $T_h$  ( $T_v$ ). To pack a module  $b_j$  in  $\Gamma_-$ , we search for the last module  $b_p$  with  $b_p \vdash b_j$  ( $b_p \perp b_j$ ) to compute the  $x$  coordinate ( $y$  coordinate) of  $b_j$ . We traverse the modules  $b_k$ 's in  $T_h$  ( $T_v$ ) from its root, and go to the right child of  $b_k$  if  $b_k \vdash b_j$  ( $b_k \perp b_j$ ). The reason to proceed to the right child is that if  $b_k \vdash b_j$  ( $b_k \perp b_j$ ), then  $x'_j \geq x'_k$  ( $y'_j \geq y'_k$ ) [the right (top) boundary of the module  $b_j$  is larger than that of the module  $b_k$ ] and thus  $b_j$  must be located in  $b_k$ 's right subtree according to the definition of a binary search tree. In contrast, we proceed to the left child if  $b_k \perp b_j$  ( $b_k \vdash b_j$ ). The process continues until a leaf position is encountered, and we make  $b_j$  the leaf node; therefore,  $x_j = x'_p$  ( $y_j = y'_p$ ), where  $b_p$  is the last module with  $b_p \vdash b_j$  ( $b_p \perp b_j$ ) in the path. (Each module is placed at a bend in the current contour, according to its geometric relationship to the placed modules defined in the constraint graphs.) As an example shown in Fig. 3(a) and (b), we make  $b_a$  the right child of  $b_s$  in  $T_h$  since  $b_s \vdash b_a$  and then  $b_b$  the left child of  $b_a$  in  $T_h$  since  $b_a \perp b_b$ , respectively.

After  $b_j$  is inserted into  $T_h$  ( $T_v$ ), every node  $b_i$  after  $b_j$  (in terms of in-order search tree order) with  $x'_i \leq x'_j$  ( $y'_i \leq y'_j$ ) in  $T_h$  ( $T_v$ ) is deleted, since  $b_i$  is no longer in the contour. For the example shown in Fig. 3(d), we delete  $b_a$  from  $T_h$  after inserting  $b_d$ , since  $x'_a \leq x'_d$  (module  $b_a$  is no longer in the horizontal contour  $T_h$ ). For another example shown in Fig. 3(g), we delete  $b_d, b_e, b_g$  (which are after  $b_f$ ) from  $T_h$  after inserting  $b_f$ , since  $x'_i \leq x'_f, i = d, e, \text{ or } g$  (module  $b_d, b_e, b_g$  are no longer in the horizontal contour  $T_h$  after  $b_f$  is inserted). It is not difficult to see that those modules [ $b_a$  in Fig. 3(d) and  $b_d, b_e, b_g$  in

<sup>2</sup>Note that, by this definition, the  $\Gamma_-$  may not always be the same as the second sequence defined in the corresponding SP. Nevertheless, both of our  $\Gamma_-$  and the second sequence of an SP are good for the efficient packing scheme introduced in this paper.

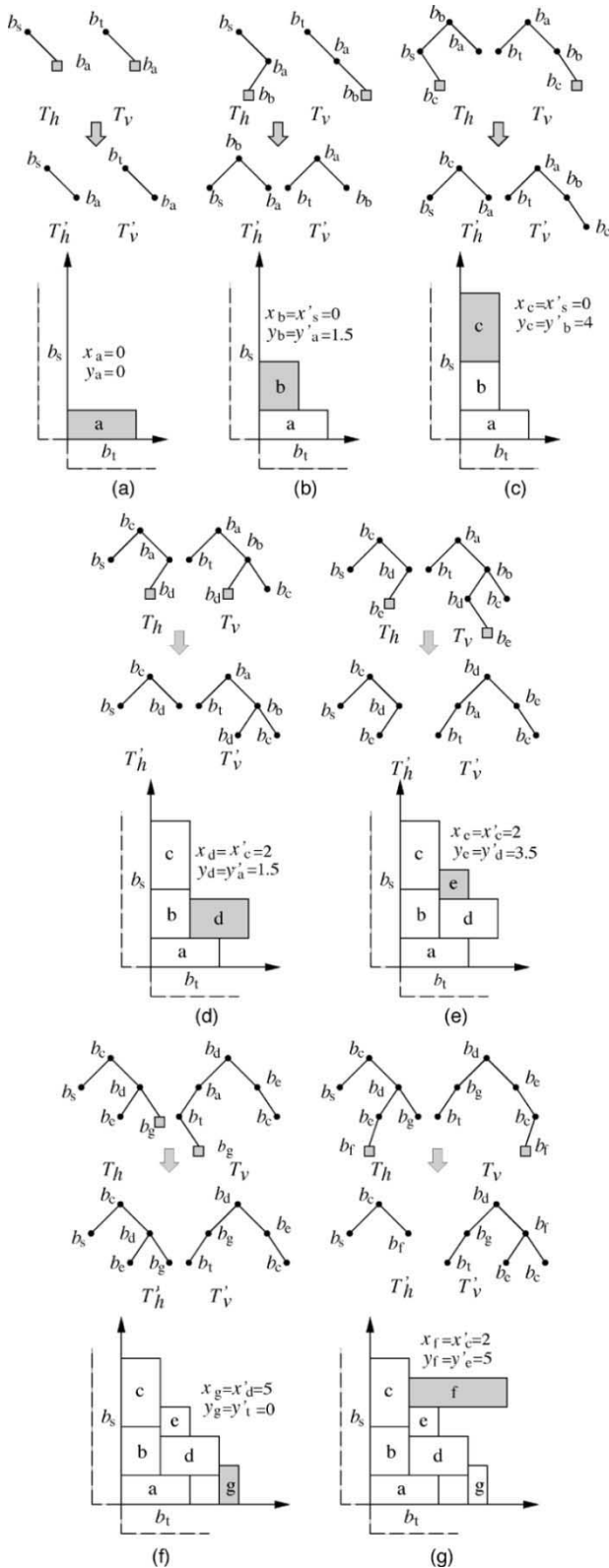


Fig. 3. Packing scheme for the TCG-S of Fig. 2(b). In each step, the red-black trees  $T_h$  and  $T_v$  corresponding to the  $R_h$  and  $R_v$  right after the module insertion, are shown.  $T'_h$  ( $T'_v$ ) gives the resulting red-black tree after removing the modules no longer in  $R_h$  ( $R_v$ ) and performing rotation to balance the tree. Note that, as a fundamental property of the binary search tree, the search-tree (in-order traversal) order is still maintained after the tree rotation.

Fig. 3(g)] are all the modules that need to be removed—the nodes  $b_p$ 's before the newly inserted node  $b_j$  in  $T_h$  all have  $x'_p \leq x_j$  since  $b_j$  must

be placed at a bend formed by two modules according to our scheme, and the remaining nodes  $b_q$ 's after  $b_j$  in  $T_h$  all have  $x'_q > x'_j$ , and thus  $b_p$ 's and  $b_q$ 's are still in the horizontal contour  $T_h$ . The situation for the vertical contour  $T_v$  can be defined analogously. In Fig. 3(d) [Fig. 3(e)], for example,  $b_c$  ( $b_d$ ) remains in  $T_h$  after  $b_d$  ( $b_e$ ) is inserted into  $T_h$  since  $x'_c \leq x_d$  ( $x'_d > x'_e$ ). This process repeats for all modules in  $\Gamma_-$ . We have  $W = x'_v$  ( $H = y'_v$ ) if  $b_v$  is the module in the resulting  $T_h$  ( $T_v$ ) with the largest value, where  $H$  ( $W$ ) denotes the height (width) of the placement.

Fig. 3 shows the packing scheme for the TCG-S of Fig. 2(g).  $T_h$  ( $T_v$ ) consists of  $b_s$  ( $b_t$ ) initially. To pack the first module  $b_a$  in  $\Gamma_-$ , we traverse  $T_h$  ( $T_v$ ) from the root  $b_s$  ( $b_t$ ) and insert it to the right child of  $b_s$  ( $b_t$ ) since  $b_s \vdash b_a$  ( $b_t \perp b_a$ ). As shown in Fig. 3(a), the first module  $b_a$  in  $\Gamma_-$  is placed at the bottom-left corner (i.e.,  $(x_a, y_a) = (0, 0)$ ) since  $b_s$  ( $b_t$ ) is the last module that is horizontally (vertically) related to  $b_a$  and  $x'_s = 0$  ( $y'_t = 0$ ). [Note that  $T'_h$  ( $T'_v$ ) in Fig. 3(a) denotes a balanced binary search tree after  $b_a$  is inserted into  $T_h$  ( $T_v$ ).] Similarly, to pack the second module  $b_b$  in  $\Gamma_-$ , we traverse  $T_h$  from the root  $b_s$  and then its right child since  $b_s \vdash b_b$ . Then,  $b_b$  is inserted to the left child of  $b_a$  since  $b_a \perp b_b$ . Because  $b_s$  is the last module with  $b_s \vdash b_b$  in the path,  $x_b = x'_s = 0$ . Similarly, we traverse  $T_v$  from the root  $b_t$  and then its right child  $b_a$  since  $b_t \perp b_a$ . Then,  $b_b$  is inserted to the right child of  $b_a$  in  $T_v$  since  $b_a \perp b_b$ . Therefore,  $y_b = y'_a = 1.5$  because  $b_a$  is the last module with  $b_a \perp b_b$  in the path. The resulting balanced binary search trees after performing tree rotations  $T'_h, T'_v$  (see [2] for the rotation operations for keeping a tree balanced), and the corresponding placement are shown in Fig. 3(b). Note that, as a fundamental property of the search tree, the tree rotation still maintain the ordering of the nodes in the search tree [2]. [See the resulting  $T'_h$  and  $T'_v$  in Fig. 3(b).] As shown in Fig. 3(c), after  $b_c$  is inserted,  $b_b$  in  $T_h$  is deleted since  $b_b$  is after  $b_c$  (in terms of in-order search tree traversal) and  $x'_b \leq x'_c$  (i.e.,  $b_b$  is no longer in the horizontal contour). The resulting  $T'_h, T'_v$ , and placement are shown in Fig. 3(c). The process is repeated for all modules in  $\Gamma_-$ , and the final  $T'_h, T'_v$ , and placement are shown in Fig. 3(g). Then, we have  $W = x'_f$  since  $b_f$  is the module with the largest  $x$  value in the final  $T'_h$ , and  $H = y'_c$  since  $b_c$  is the module with the largest  $y$  value in the final  $T'_v$ .

According to this packing scheme, if the coordinate of a module  $b_i$  in  $\Gamma_-$  is changed, we only need to recompute the coordinates of modules after  $b_i$  in  $\Gamma_-$ , since the coordinates of modules before  $b_i$  do not change.

The above packing scheme leads to the following theorem and lemmas.

**Theorem 2:** There exists a unique placement corresponding to a TCG-S.

*Proof:* As shown in Section III-B, TCG-S is equivalent to TCG and SP. Since there exists a unique placement corresponding to a TCG [9] (or an SP [13]), there exists a unique placement corresponding to a TCG-S. (The above packing scheme provides a faster approach to determining the coordinate for each module.) ■

**Theorem 3:** The size of the solution space for TCG-S =  $(C_h, C_v, \Gamma_-)$  is  $(m!)^2$ , where  $m$  is the number of modules.

*Proof:* The sequence  $\Gamma_-$  is the topological order of both  $C_h$  and  $C_v$  and is thus uniquely determined by  $C_h$  and  $C_v$ . Therefore, the solution space of TCG-S is the same as that of TCG, which is  $(m!)^2$  [9], where  $m$  is the number of modules. ■

**Lemma 1:** For each module  $b_j$  in  $\Gamma_-$ ,  $b_j$  must be placed adjacent to the right (top) boundary of some module  $b_i$  in  $R_h$  ( $R_v$ ) during the packing.

*Proof:* For a placed module  $b_k$ , if  $b_k$  is not in  $R_h$ , there must exist a placed module  $b_l$  above  $b_k$  whose right boundary is larger than that of  $b_k$  (i.e.,  $x'_l > x'_k$  and  $y_l \geq y'_k$ ). Since  $b_l$  is placed before  $b_j$ ,  $\Gamma_-$  is

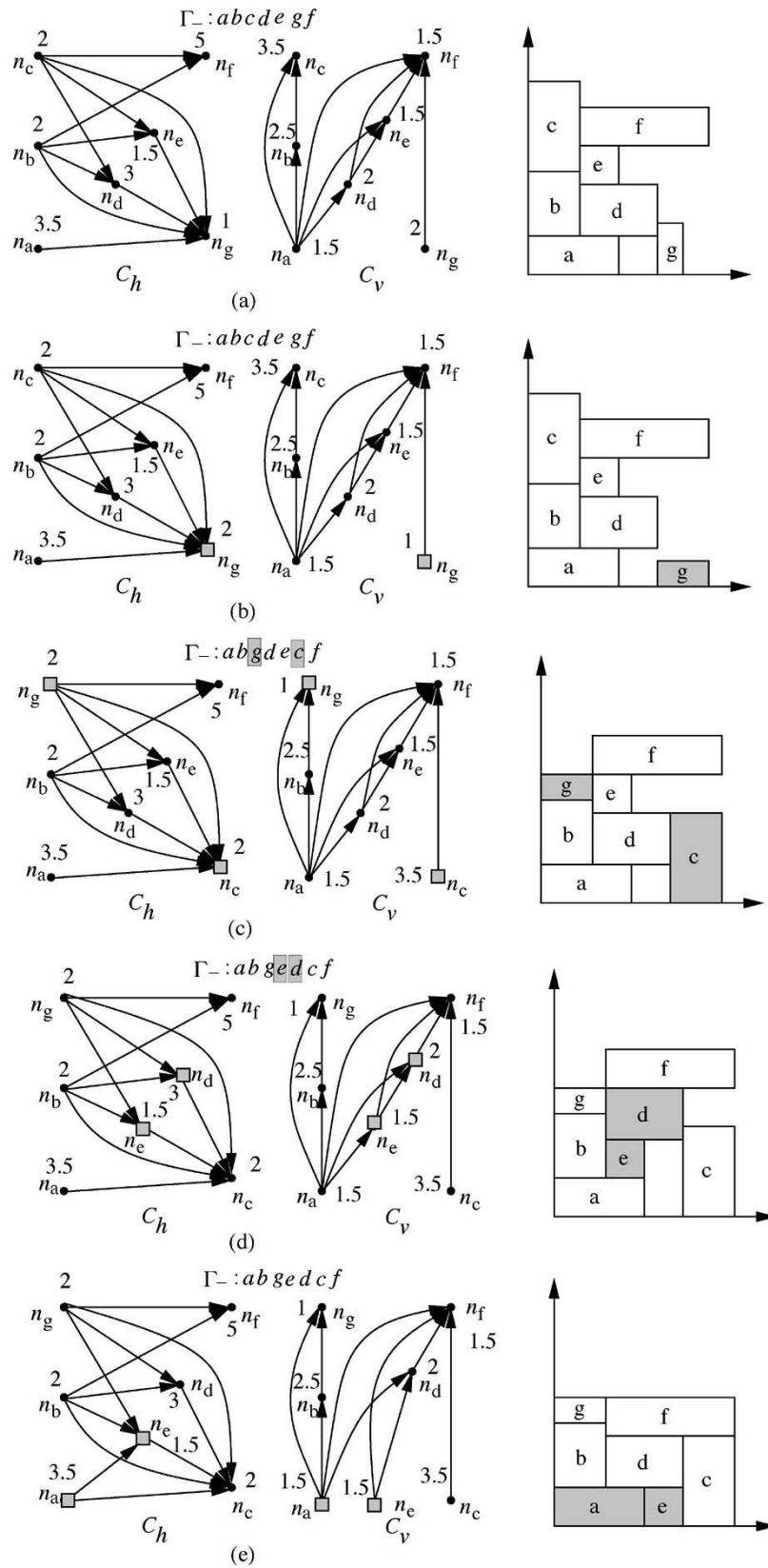


Fig. 4. Four types of perturbation. (a) The initial TCG-S and placement. (b) The resulting TCG-S and placement after rotating the module  $b_g$  shown in (a). (c) The resulting TCG-S and placement after swapping the nodes  $n_c$  and  $n_g$  shown in (b). (d) The resulting TCG-S and placement after reversing the reduction edge  $(n_d, n_e)$  shown in (c). (e) The resulting TCG-S and placement after moving the reduction edge  $(n_a, n_e)$  from the  $C_v$  of (d) to  $C_h$ .

of the sequence  $\langle \dots l \dots i \dots \rangle$ . If  $b_j$  is adjacent to the right boundary of  $b_k$ ,  $b_j$  should also be below  $b_l$ . This implies that there exists an edge of  $\langle \dots l \dots j \dots \rangle$  (a contradiction). Therefore,  $b_j$  must be adjacent to

some module  $b_i$  in current  $R_h$ . Similarly,  $b_j$  must be placed above some module in  $R_v$  during packing. ■

**Lemma 2:** Given a module  $b_j$  in  $\Gamma_-$  to be placed, if  $b_i \in R_h(R_v)$  and  $b_i \perp b_j$  ( $b_i \vdash b_j$ ), any module  $b_k \in R_h(R_v)$  with  $x'_k > x'_i$  ( $y'_k > y'_i$ ) cannot bear the relation  $b_k \vdash b_j$  ( $b_k \perp b_j$ ).

**Proof:** Suppose there exists a module  $b_k$  in  $R_h$  so that  $x'_k > x'_i$  and  $b_k \vdash b_j$ , when we determine the  $x$  coordinate of a module  $b_j$ . The relation between  $b_i$  and  $b_k$  can be either  $b_i \vdash b_k$  (since  $x'_i < x'_k$ ) or  $b_k \perp b_i$  (since  $b_i$  would have been removed from  $R_h$  if  $b_i \perp b_k$ ). If  $b_i \vdash b_k$ , then  $b_i \vdash b_j$  since  $b_k \vdash b_j$  (based on Property 3 of TCG-S), contradicting Property 2 of TCG-S because there are two geometric relations  $b_i \vdash b_j$  and  $b_i \perp b_j$  between  $b_i$  and  $b_j$ . Similarly, if  $b_k \perp b_i$ , then  $b_k \perp b_j$  since  $b_i \perp b_j$ , contradicting Property 2 of TCG-S because  $b_k \vdash b_j$  and  $b_k \perp b_j$ . Similar claims hold for  $R_v$ . ■

By this lemma, during the packing for the module  $b_j$ , if  $b_i \in R_h$  and  $b_i \perp b_j$ , then any module  $b_k \in R_h$  after  $b_i$  (in the search-tree order) cannot have the relation  $b_k \vdash b_j$ . It is clear later that this lemma is useful for searching for the last module  $b_p$  with  $b_p \vdash b_j$  for computing the coordinate of  $b_j$ —if  $b_i \in R_h$  and  $b_i \perp b_j$ , every module  $b_k \in R_h$  after  $b_i$  can be discarded during the search.

For each module  $b_j$ , its  $x$  coordinate  $x_j$  equals the maximum  $x'_k$  (the largest right boundary) among those modules  $b_k$ 's with  $b_k \vdash b_j$  in TCG-S. Based on Lemma 1,  $b_k$  must be in  $R_h$ . Therefore, we only need to traverse the modules in  $R_h$  to find such a module. Since modules in  $R_h$  are stored in a balanced binary search tree  $T_h$ , the traversal from its root to a leaf takes only  $O(\lg m)$  time, where  $m$  is the number of nodes (modules). For each module  $b_p$  encountered, we go to its right child if  $b_p \vdash b_j$  since  $b_p$ 's right child corresponds to some module  $b_u$  with  $x'_u \geq x'_p$  based on the definition of our search-tree order. Note that our goal is to find the module  $b_k$  with the largest right boundary such that  $b_k \vdash b_j$ ; if such a module is found, then  $x_j = x'_k$  and we have obtained the  $x$  coordinate of the module  $x_j$ . However, if  $b_p \perp b_j$ , we traverse the left child of  $b_p$ . By Lemma 2, the modules  $b_q$ 's after  $b_p$  (in the search-tree order) cannot bear the relation  $b_q \vdash b_j$  if  $b_p \perp b_j$ ; therefore, we do not need to consider the right subtree of  $b_p$  for this case. As the example shown in Fig. 3(e) for the computation of the  $x$  coordinate of the module  $e$ , we traverse the right child of the root  $b_c$  since  $b_c \vdash b_e$ , and then make  $b_e$  the left child of  $b_d$  since  $b_d \perp b_e$ . Therefore, we are done with the traversal, and  $x_e = x'_c$  since  $b_c$  has the maximum right boundary among the modules horizontally related to  $b_e$ . For the example shown in Fig. 3(f) for the computation of the  $x$  coordinate of the module  $g$ , we traverse the right child  $b_d$  of the root  $b_c$  since  $b_c \vdash b_g$ , and then make  $b_g$  the right child of  $b_d$  since  $b_d \vdash b_g$ . We therefore make  $x_g = x'_d$  since  $b_d$  is the module with the largest right boundary such that  $b_d \vdash b_g$ . Note that we do not need to consider  $b_e$  in this case, since it is before  $b_d$  in the search tree, implying that  $b_e$ 's right boundary is not larger than that of  $b_d$ . By repeating this procedure,  $x_j$  equals  $x'_r$  if  $b_r$  is the last module in the search path with  $b_r \vdash b_j$ . A similar process can be applied to compute the  $y$  coordinate of module  $b_i$ . We have the following theorem.

**Theorem 4:** The proposed scheme correctly packs all modules in  $O(m \lg m)$  time, where  $m$  is the number of modules.

**Proof:** For each module  $b_j$ , its  $x$  coordinate  $x_j$  equals the maximum  $x'_k$  among those modules  $b_k$ 's with  $b_k \vdash b_j$  in TCG-S. Based on Lemma 1,  $b_k$  must be in  $R_h$ . Therefore, we only need to traverse the modules in  $R_h$  to find such a module. Since the modules in  $R_h$  are stored in a balanced tree  $T_h$  with the search-tree order defined on the right boundaries of the modules, the traversal can be done from its root to a leaf. For each module  $b_p$  encountered, we go to its right child if  $b_p \vdash b_j$  since  $b_p$ 's right child corresponds to some module  $b_u$  with  $x'_u \geq x'_p$  based on the definition of our search-tree order. Note that our goal is to find the module  $b_k$  with the largest right boundary such

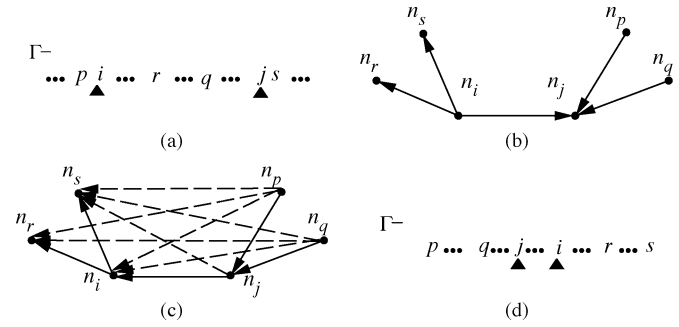


Fig. 5. Example of updating  $\Gamma_-$  by reversing an edge  $(n_i, n_j)$ . (a)  $\Gamma_-$  before the operation. (b) A constraint graph before the operation. (c) The new constraint graph after the operation. (d) The new  $\Gamma_-$  after the operation.

that  $b_k \vdash b_j$ ; if such a module is found, then  $x_j = x'_k$  and we have obtained the  $x$  coordinate of the module  $x_j$ . However, if  $b_p \perp b_j$ , we traverse the left child of  $b_p$ . By Lemma 2, the modules  $b_q$ 's after  $b_p$  (in the search-tree order) cannot bear the relation  $b_q \vdash b_j$  if  $b_p \perp b_j$ ; therefore, we do not need to consider the right subtree of  $b_p$ . By repeating this procedure,  $x_j$  equals  $x'_r$  if  $b_r$  is the last module in the search path with  $b_r \vdash b_j$ . Similar claim holds for the process to get the  $y$  coordinate of module  $b_i$  in  $R_v$ .

For any module  $b_p \in R_h$ , either  $b_p \vdash b_j$  or  $b_p \perp b_j$ , since we place  $b_j$  at the bend formed by two modules in the horizontal contour. Therefore, we only need to search for a path from the root to a leaf to pack a module. For a balanced binary tree with  $n$  nodes, the path length is given by the height of the tree, which is  $O(\lg n)$ . The time complexity of inserting and deleting a node in the tree is  $O(\lg n)$ . Therefore, the time complexity of our packing scheme is given by

$$O\left(\sum_{i=1}^m \lg i + \sum_{i=1}^m \lg i\right) = O(m \lg m)$$

where the first and the second terms correspond to the time complexity of inserting and deleting nodes into the tree, respectively. ■

## V. FLOORPLANNING ALGORITHM

We develop a simulated annealing-based algorithm [6] by using TCG-S for nonslicing floorplan design. Given an initial TCG-S, the algorithm perturbs the TCG-S into a new TCG-S to find a desired solution. To ensure the correctness of the new  $C_h$  and  $C_v$ , they must satisfy the three feasibility conditions given in Section III-A. To identify feasible  $C_h$  and  $C_v$  for perturbation, we describe the concept of *reduction edges* in the following subsection.

### A. Reduction Edge

An edge  $(n_i, n_j)$  is said to be a *reduction edge* if there does not exist another path from  $n_i$  to  $n_j$ , except the edge  $(n_i, n_j)$  itself; otherwise, it is a *closure edge*. In Fig. 2(g), for example, edges  $(n_a, n_g)$ ,  $(n_d, n_g)$ , and  $(n_e, n_g)$  are reduction edges while  $(n_b, n_g)$  and  $(n_c, n_g)$  are closure ones. With  $\Gamma_-$ , we can find a set of reduction edges in  $O(m)$  time (where  $m$  is the number of modules), a significant improvement from  $O(m^2)$  time using TCG alone [9].

Given an arbitrary node  $n_i$  in a transitive closure graph  $C_h$  ( $C_v$ ), we can find all the nodes  $n_j$ 's that form reduction edges  $(n_i, n_j)$ 's using a *Linear Scan* method as follows. First, we extract from  $\Gamma_-$  those nodes  $n_j$ 's in  $F_{\text{out}}(n_i)$  of  $C_h$  ( $C_v$ ) and keep their original ordering in  $\Gamma_-$ . Let the resulting sequence be  $S$ . The first node  $n_k$  in  $S$  and  $n_i$  must form a reduction edge  $(n_i, n_k)$ . Then, we continue to traverse  $S$  until a node  $n_l$  with  $(n_k, n_l)$  not in  $C_h$  ( $C_v$ ) is encountered.  $(n_i, n_l)$  must also be

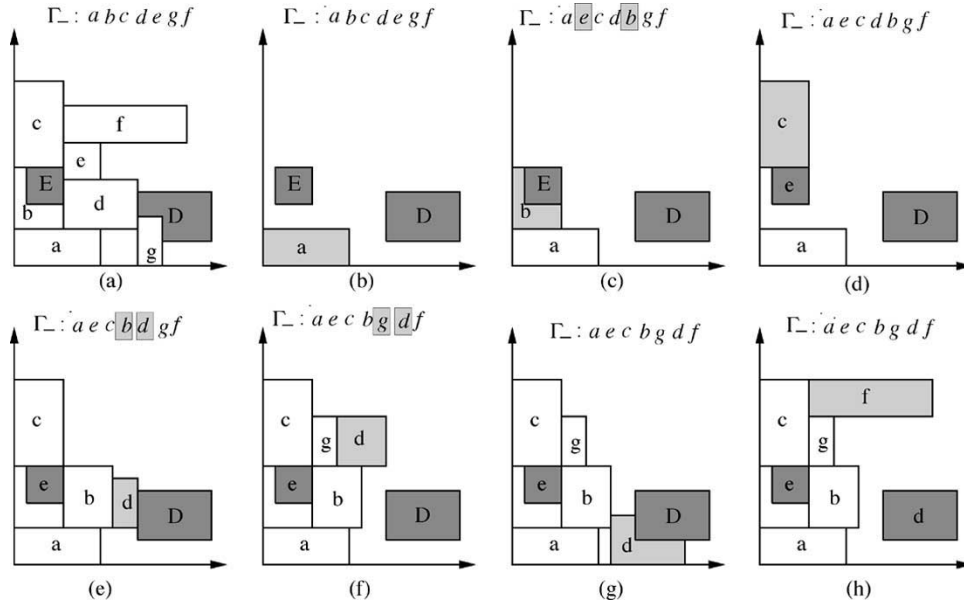


Fig. 6. Examples for preplaced modules. (a) The resulting placement of TCG-S shown in Fig. 2(g). Here, the heavily shaded rectangles  $D$  and  $E$  denote the preplaced locations for  $b_d$  and  $b_e$ . (b)–(h) The process to transform an infeasible TCG-S into a feasible one.

a reduction edge. Starting from  $n_l$ , we continue the same process until no node is left in  $S$ .

As an example shown in  $C_h$  of Fig. 2(g), we are to extract all reduction edges emanating from  $n_c$ . We first find  $S = \langle n_d, n_e, n_g, n_f \rangle$  by extracting nodes in  $F_{out}(n_c)$  based on the sequence in  $\Gamma_-$ .  $n_c$  and the first node  $n_d$  in  $S$  form a reduction edge  $(n_c, n_d)$ . Traversing  $S$ , we have another reduction edge  $(n_c, n_e)$  since edge  $(n_d, n_e)$  is not in  $C_h$ . Starting from  $n_e$ , we search the next node  $n$  with  $(n_e, n)$  not in  $C_h$ . We find node  $n_f$ , implying  $(n_c, n_f)$  is also a reduction edge. Therefore, we have found all reduction edges emanating from  $n_c$ :  $(n_c, n_d)$ ,  $(n_c, n_e)$ , and  $(n_c, n_f)$ . (Note that  $(n_c, n_g)$  is not a reduction edge, because we found  $(n_e, n_g)$  in  $C_h$  during the processing.)

**Theorem 5:** Given a node  $n_i$  in  $C_h$  ( $C_v$ ), the Linear Scan method finds all reduction edges emanating from  $n_i$  in  $O(m)$  time, where  $m$  is the number of modules.

*Proof:* Given an arbitrary node  $n_i$  in a transitive closure graph  $C_h$  ( $C_v$ ), we first extract those nodes  $n_j$ 's in  $F_{out}(n_i)$  by scanning modules in  $\Gamma_-$ . Let the resulting sequence be  $S$ .  $n_i$  and the first node  $n_k$  in  $S$  must form a reduction edge  $(n_i, n_k)$ . If  $(n_i, n_k)$  is a closure edge, there must exist a node  $n_p$  in the path  $\langle n_i, \dots, n_p, \dots, n_k \rangle$  from  $n_i$  to  $n_k$  in  $C_h$  ( $C_v$ ), implying that  $n_p$  must be extracted before  $n_k$  in the scanning (contradicting the fact that  $n_k$  is the first node encountered in  $\Gamma_-$ ). Therefore,  $(n_i, n_k)$  is a reduction edge. Then, we continue traversing nodes in  $S$  until another node  $n_l$  associated with edge  $(n_k, n_l)$  not in  $C_h$  ( $C_v$ ) is met. For those nodes,  $n_q$ 's between  $n_k$  and  $n_l$ ,  $(n_i, n_q)$  must be a closure edge since there exists a path  $\langle n_i, n_k, \dots, n_q \rangle$  from  $n_i$  to  $n_q$  in  $C_h$  ( $C_v$ ). However, nodes  $n_i$  and  $n_l$  form a reduction edge. If there exists a path from  $n_i$  to  $n_l$ , the path must pass through at least one node  $n_q$  between  $n_k$  and  $n_l$  in  $S$ . However,  $n_q$  is connected by  $n_k$ , implying the existence of the path  $\langle n_k, n_q, n_l \rangle$ . According to Property 3 of TCG, the edge  $(n_k, n_l)$  also exists (a contradiction). Therefore,  $n_i$  and  $n_l$  form a reduction edge  $(n_i, n_l)$ . The same process continues for node  $n_l$ .

For a successor node  $n_r$  of  $n_l$ , if edge  $(n_l, n_r)$  exists in  $C_h$  ( $C_v$ ), edge  $(n_i, n_r)$  must be the closure edge according to the above reasoning. If the edge  $(n_l, n_r)$  does not exist in  $C_h$  ( $C_v$ ), we show that  $n_r$  cannot connect to a node  $n_v$ , where  $n_v$  is the node before  $n_l$  in  $S$ . Suppose that the edge  $(n_l, n_r)$  does not exist in  $C_h$  ( $C_v$ ), but  $n_r$  is connected to node  $n_v$ , where  $n_v$  is the node before  $n_l$  in  $S$  and the

TABLE I  
FIVE MCNC BENCHMARK CIRCUITS

Circuit	# of modules	# of I/O pads	# of nets	# of pins
apte	9	73	97	214
xerox	10	107	203	696
hp	11	43	83	264
ami33	33	42	123	480
ami49	49	24	408	931

edge  $(n_i, n_v)$  is a reduction edge. [If  $(n_i, n_v)$  is a closure edge, we can always find another node  $n_u$  that is a fanin of  $n_v$  and  $(n_i, n_u)$  is a reduction edge.] If  $(n_i, n_v)$  and  $(n_i, n_l)$  are reduction edges in  $C_h$  ( $C_v$ ), there must exist an edge  $(n_v, n_l)$  in  $C_v$  ( $C_h$ ) since there exists a unique edge between each pair of nodes in TCG. Similarly, because the edge  $(n_l, n_r)$  does not exist in  $C_h$  ( $C_v$ ), the edge  $(n_l, n_r)$  must exist in  $C_v$  ( $C_h$ ). The path  $\langle n_v, n_l, n_r \rangle$  exists in  $C_v$  ( $C_h$ ), implying that the edge  $(n_v, n_r)$  also exists in  $C_v$  ( $C_h$ ). Therefore, the edge  $(n_v, n_r)$  exists in both  $C_h$  and  $C_v$ , contradicting Property 2 of TCG.

It takes  $O(m)$  time to scan modules in  $\Gamma_-$  to find nodes  $n_j$ 's that belong to  $F_{out}(n_i)$ . Therefore, the Linear Scan method finds all reduction edges emanating from  $n_i$  in  $O(m)$  time, where  $m$  is the number of modules. ■

## B. Solution Perturbation

We extend the four operations *rotation*, *swap*, *reverse*, and *move* presented in [9] to perturb  $C_h$  and  $C_v$ . During each perturbation, we must maintain the three feasibility properties for  $C_h$  and  $C_v$ . Unlike the rotation operation, swap, reverse, and move may change the configurations of  $C_h$  and  $C_v$  and thus their properties. Further, we also need to maintain  $\Gamma_-$  to conform to the topological ordering for new  $C_h$  and  $C_v$ .

1) *Rotation:* To rotate a module  $b_i$ , we exchange the weights of the corresponding node  $n_i$  in  $C_h$  and  $C_v$ . Since the configurations of  $C_h$  and  $C_v$  do not change, so does  $\Gamma_-$ . Fig. 4(b) shows the resulting TCG-S and placement after rotating the module  $g$  shown in Fig. 4(a). Notice that the new  $\Gamma_-$  is the same as that in Fig. 4(a).

**Theorem 6:** TCG-S is closed under the rotation operation, and such an operation does not change the topology of the TCG and  $\Gamma_-$ .



TABLE II

AREA AND RUNTIME COMPARISONS AMONG SP (ON SUN SPARC ULTRA60), O-TREE (ON SUN SPARC ULTRA 60), B\*-TREE (ON SUN SPARC ULTRA-I), ENHANCED O-TREE (ON SUN SPARC ULTRA60), CBL (ON SUN SPARC 20), TCG (ON SUN SPARC ULTRA60) AND TCG-S (ON SUN SPARC ULTRA60) FOR AREA OPTIMIZATION

Circuit	SP		O-tree		B*-tree		Enhanced O-tree		CBL		TCG		TCG-S	
	Area (mm <sup>2</sup> )	Time (sec)	Area (mm <sup>2</sup> )	Time (sec)	Area (mm <sup>2</sup> )	Time (sec)	Area (mm <sup>2</sup> )	Time (sec)	Area (mm <sup>2</sup> )	Time (sec)	Area (mm <sup>2</sup> )	Time (sec)	Area (mm <sup>2</sup> )	Time (sec)
apte	48.12	13	47.1	38	46.92	7	46.92	11	NA	NA	46.92	1	46.92	1
xerox	20.69	15	20.1	118	19.83	25	20.21	38	20.96	30	19.83	18	19.796	5
hp	9.93	5	9.21	57	8.947	55	9.16	19	(66.14)	(32)	8.947	20	8.947	7
ami33	1.22	676	1.25	1430	1.27	3417	1.24	118	1.20	36	1.20	306	1.185	84
ami49	38.84	1580	37.6	7428	36.80	4752	37.73	406	38.58	65	36.77	434	36.398	369

*Proof:* The configuration of TCG is not changed after a rotation operation, neither is  $\Gamma_-$ . ■

2) *Swap:* Swapping  $n_i$  and  $n_j$  does not change the topologies of  $C_h$  and  $C_v$ . Therefore, we only need to exchange  $b_i$  and  $b_j$  in  $\Gamma_-$ . Fig. 4(c) shows the resulting TCG-S and placement after swapping the nodes  $n_c$  and  $n_g$  shown in Fig. 4(b). Notice that the modules  $b_c$  and  $b_g$  in  $\Gamma_-$  in Fig. 4(c) are exchanged.

*Theorem 7:* TCG-S is closed under the Swap operation, and such an operation takes  $O(1)$  time.

*Proof:* The Swap operation only exchanges two nodes  $n_i$  and  $n_j$  in both  $C_h$  and  $C_v$  without changing their topologies. Therefore, we only need to exchange two nodes in  $\Gamma_-$ , which takes  $O(1)$  time. ■

3) *Reverse:* To reverse a reduction edge  $(n_i, n_j)$  in one transitive closure graph, we first delete the edge  $(n_i, n_j)$  from the graph, and then add the edge  $(n_j, n_i)$  to the graph. To keep  $C_h$  and  $C_v$  feasible, for each node  $n_k \in F_{in}(n_j) \cup \{n_j\}$  and  $n_l \in F_{out}(n_i) \cup \{n_i\}$  in the new graph, we have to keep the edge  $(n_k, n_l)$  in the new graph. If the edge does not exist in the graph, we add the edge to the graph and delete the corresponding edge  $(n_k, n_l)$  [or  $(n_l, n_k)$ ] in the other graph. To make  $\Gamma_-$  conform to the topological ordering of new  $C_h$  and  $C_v$ , we delete  $b_i$  from  $\Gamma_-$  and insert  $b_i$  after  $b_j$ . For each module  $b_k$  between  $b_i$  and  $b_j$  in  $\Gamma_-$ , we shall check whether the edge  $(n_i, n_k)$  exists in the same graph. We do nothing if the edge  $(n_i, n_k)$  does not exist in the same graph; otherwise, we delete  $b_k$  from  $\Gamma_-$  and insert it after the most recently inserted module.

Fig. 4(d) shows the resulting TCG-S and placement after reversing the reduction edge  $(n_d, n_e)$  of the  $C_v$  in Fig. 4(c). Since there exists no module between  $b_d$  and  $b_e$  in  $\Gamma_-$ , we only need to delete  $b_d$  from  $\Gamma_-$  and insert it after  $b_e$ , and the resulting  $\Gamma_-$  is shown in Fig. 4(d).

*Theorem 8:* TCG-S is closed under the Reverse operation, and such an operation takes  $O(m)$  time, where  $m$  is the number of modules.

*Proof:* If an edge  $(n_i, n_j)$  in  $C_h$  ( $C_v$ ) is reversed, the Reverse operation will add some edges  $(n_k, n_l)$ 's to  $C_h$  ( $C_v$ ) and delete the corresponding edges in  $C_v$  ( $C_h$ ), where  $n_k \in F_{in}(n_j) \cup \{n_j\}$  and  $n_l \in F_{out}(n_i) \cup \{n_i\}$ .  $\Gamma_-$  is changed because the topological ordering of nodes is changed by those newly added edges. To show the effects of the operation, without loss of generality, we consider  $\Gamma_-$  of the form shown in Fig. 5(a), where: 1)  $p$  is a module before module  $i$  and  $n_p$  is a fanin of  $n_j$  (since Reverse only adds edges that start from  $n_k$ 's, where  $n_k \in F_{in}(n_j) \cup \{n_j\}$ , we do not need to consider the case where  $n_p$  is a fanin of  $n_i$ ); 2)  $q$  and  $r$  are modules between modules  $i$  and  $j$ , and  $n_q$  is a fanin of  $n_j$ , while  $n_r$  is a fanout of  $n_i$  [note that if  $n_q$  or  $n_r$  is a fanout of  $n_i$  or a fanin of  $n_j$ , edge  $(n_i, n_j)$  must be a closure edge (a contradiction)]; and 3)  $s$  is a module after module  $j$ , and  $n_s$  is a fanout of  $n_i$  (since Reverse only adds edges that end in  $n_l$ 's, where  $n_l \in F_{out}(n_i) \cup \{n_i\}$ , we do not need to consider the case where  $n_s$  is a fanout of  $n_j$ ). See Fig. 5(b) for the corresponding  $C_h$  ( $C_v$ ). The resulting  $C_h$  ( $C_v$ ) after the operation is shown in Fig. 5(c), in which the dotted lines denote newly added edges. For edges  $(n_p, n_r)$ ,  $(n_p, n_i)$ , and  $(n_p, n_s)$  [( $n_j, n_r$ ), ( $n_j, n_i$ ), and ( $n_j, n_s$ )] starting from  $n_p$  ( $n_j$ ), the topological ordering of nodes in the edges is not changed [i.e.,

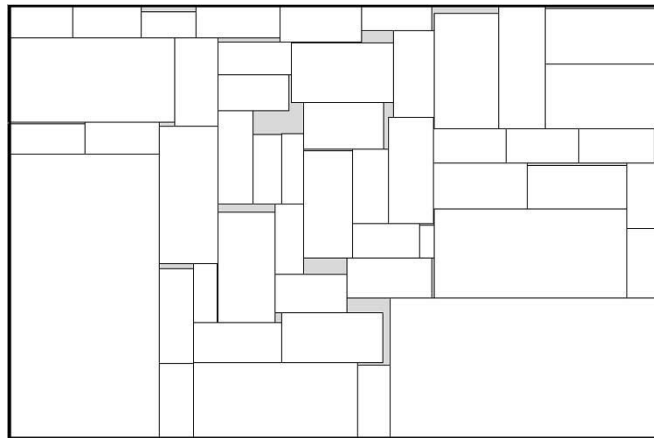


Fig. 7. Resulting placement of ami49 with area optimization (area = 36.398 mm<sup>2</sup>).

$n_p$  ( $n_j$ ) is in front of  $n_r$ ,  $n_i$ , or  $n_s$ ]. However, for some edges  $(n_q, n_r)$  and  $(n_q, n_i)$  starting from  $n_q$ , the topological ordering of nodes in the edges is reversed (i.e.,  $n_q$  is in front of  $n_i$  ( $n_r$ ) instead of behind them). Therefore, we only need to move module  $i$  and those modules between modules  $i$  and  $j$  that belong to the fanout of  $n_i$  after module  $j$  in  $\Gamma_-$ . Fig. 5(d) shows the new  $\Gamma_-$  after the operation. The number of modules between modules  $i$  and  $j$  is at most  $m - 2$ ; therefore, it takes  $O(m)$  time to move these modules after  $b_j$ . ■

4) *Move:* To move a reduction edge  $(n_i, n_j)$  from a transitive closure graph  $G$  to the other  $G'$ , we delete the edge from  $G$  and then add it to  $G'$ . Similar to Reverse, for each node  $n_k \in F_{in}(n_i) \cup \{n_i\}$  and  $n_l \in F_{out}(n_j) \cup \{n_j\}$  in  $G'$ , we must move the edge  $(n_k, n_l)$  to  $G'$  if the corresponding edge  $(n_k, n_l)$  (or  $(n_l, n_k)$ ) is in  $G$ . Since the operation changes only the edges in  $C_h$  or  $C_v$  but not the topological ordering among nodes,  $\Gamma_-$  remains unchanged.

Fig. 4(e) shows the resulting TCG-S and placement after moving the reduction edge  $(n_a, n_e)$  from  $C_v$  to  $C_h$  in Fig. 4(d). Notice that the resulting  $\Gamma_-$  is the same as that in Fig. 4(d). For the above operations, we have the following theorem.

*Theorem 9:* TCG-S is closed under the move operation, and such an operation takes  $O(m)$  time, where  $m$  is the number of modules. In particular,  $\Gamma_-$  remains the same after the operation.

As shown in [5], in particular, the aforementioned operations form a complete set of operations for perturbing a TCG, i.e., every feasible TCG is reachable from any other feasible TCG. Since  $\Gamma_-$  is induced from TCG, the set of perturbation operations is also sufficient for TCG-S.

## VI. PLACEMENT WITH CONSTRAINTS

In this section, we demonstrate the flexibility of TCG-S by extending it to handle placement with boundary and preplaced modules.

TABLE III  
WIRELENGTH AND RUNTIME COMPARISONS AMONG O-TREE, ENHANCED O-TREE, TCG, AND TCG-S FOR  
WIRELENGTH OPTIMIZATION. ALL RAN ON SUN SPARC ULTRA60

Circuit	O-tree		enhanced O-tree		TCG		TCG-S	
	Wire (mm)	Time (sec)	Wire (mm)	Time (sec)	Wire (mm)	Time (sec)	Wire (mm)	Time (sec)
apte	317	47	317	15	363	2	363	2
xerox	368	160	372	39	366	15	366	6
hp	153	90	150	19	143	10	143	4
ami33	52	2251	52	177	44	52	43	89
ami49	636	14112	629	688	604	767	579	570

#### A. TCG-S With Boundary Modules

The placement with boundary constraints is to place a set of prespecified modules along the designated boundaries of a chip, which can be formulated as follows:

*Definition 1: Boundary Constraint:* Given a boundary module  $b$ , it must be placed in one of the four sides: on the left, on the right, at the bottom or at the top in a chip in the final packing.

TCG-S keeps the following properties that make placement with boundary constraints much easier than other representations.

*Theorem 10:* If a module  $b_i$  is placed along the left (right) boundary, the in-degree (out-degree) of the node  $n_i$  in  $C_h$  equals zero. If a module  $b_i$  is placed along the bottom (top) boundary, the in-degree (out-degree) of node  $n_i$  in  $C_v$  equals zero.

*Proof:* If the in-degree of a node  $n_i$  in  $C_h$  is zero, there exists no module on the left side of  $b_i$  in the corresponding placement. Therefore,  $b_i$  is always placed along the left boundary after packing. If the out-degree of a node  $n_i$  in  $C_h$  is zero, there exists no module on the right side of  $b_i$  in the corresponding placement. Therefore, we can push the module to the right boundary by assigning its  $x$  coordinate as  $W - W_i$ , where  $W$  is the width of the placement. Similar claims hold for the bottom and top boundary modules. ■

For each perturbation, we can guarantee a feasible placement by checking whether the conditions of boundary modules are satisfied. We discuss the modifications for the four perturbation operations as follows.

1) *Rotation:* Since Rotation does not change module location, the operation remains the same as before.

2) *Swap:* We can swap two nodes  $n_a$  and  $n_b$  if

- 1)  $b_a$  and  $b_b$  are not boundary modules,
- 2)  $b_a$  and  $b_b$  are boundary modules of the same type, or
- 3)  $b_a$  is a boundary module and  $b_b$  is not, and  $n_b$  satisfies the boundary constraint of  $b_a$ .

3) *Reverse:* If  $b_a$  is a left boundary module or  $b_b$  is a right boundary module, then the reduction edge  $(n_a, n_b)$  in  $C_h$  cannot be reversed. Similarly, we cannot reverse the reduction edge  $(n_a, n_b)$  in  $C_v$  if  $b_a$  is a bottom boundary module or  $b_b$  is a top boundary module.

4) *Move:* If  $b_a$  is a top boundary module or  $b_b$  is a bottom boundary module, we cannot move the reduction edge  $(n_a, n_b)$  from  $C_h$  to  $C_v$ . Similarly, we cannot move the reduction edge  $(n_a, n_b)$  from  $C_v$  to  $C_h$  if  $b_a$  is a right boundary module or  $b_b$  is a left boundary module.

We have the following theorem.

*Theorem 11:* TCG-S is closed under the rotation, swap, reverse, and move operations with boundary constraints.

*Proof:* To show TCG-S is closed under the rotation, swap, reverse, and move operations with boundary constraints, we only need to prove that the feasibility conditions of boundary modules defined in Theorem 10 are not violated under these operations.

- *Rotation:* Since the rotation operation does not change the configuration of TCG-S, the feasibility conditions of boundary modules are not violated.

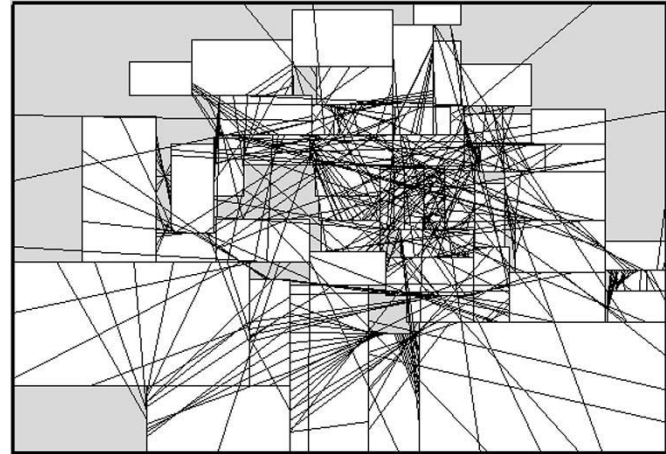


Fig. 8. Resulting placement of ami49 with wirelength optimization (wire = 579 mm).

- *Swap:* If a boundary module  $b_i$  and another module  $b_j$  are exchanged in the Swap operation, the feasible condition of the boundary module  $b_i$  is checked before the operation. Therefore, Theorem 10 is not violated under the swap operation.
- *Reverse:* If an edge  $(n_i, n_j)$  in  $C_h$  ( $C_v$ ) is reversed, the reverse operation will add some edges  $(n_k, n_l)$ 's to  $C_h$  ( $C_v$ ) and delete the corresponding edges in  $C_v$  ( $C_h$ ), where  $n_k \in F_{in}(n_j) \cup \{n_j\}$  and  $n_l \in F_{out}(n_i) \cup \{n_i\}$ . We first consider the feasibility condition of the top (bottom, left, or right) module if a reduction edge in  $C_h$  is reversed as follows: Since the reverse operation does not add any edge to  $C_v$  if an edge  $(n_i, n_j)$  in  $C_h$  is reversed, it will not generate any new edge associated with the fanin (fanout) of a bottom (top) module in  $C_v$ . Therefore, the feasibility condition of the bottom (top) module is not violated. For a left boundary module  $b_q$ , suppose there exists an edge  $(n_p, n_q)$  in  $C_h$  after the operation.  $n_q$  is either  $n_i$  or a fanout of  $n_i$ . However, we do not reverse the edge  $(n_i, n_j)$  in  $C_h$  if  $n_i$  is a left boundary module. Besides,  $n_q$  cannot be a fanout of others in the original graph  $C_h$  if  $b_q$  is a left boundary. Similarly, for a right boundary module  $b_p$ , suppose there exists an edge  $(n_p, n_q)$  in  $C_h$  after the operation.  $n_p$  is either  $n_j$  or a fanin of  $n_j$ . However, we do not reverse an edge  $(n_i, n_j)$  in  $C_h$  if  $n_j$  is a right boundary module. Besides,  $n_p$  cannot be fanin of others in the original graph  $C_h$  if  $b_p$  is a right boundary module. Similar claims hold when an edge  $(n_i, n_j)$  in  $C_v$  is reversed.
- *Move:* If an edge  $(n_i, n_j)$  in  $C_h$  ( $C_v$ ) is moved to  $C_v$  ( $C_h$ ), the Move operation will add some edges  $(n_k, n_l)$ 's to  $C_v$  ( $C_h$ ) and delete the corresponding edges in  $C_h$  ( $C_v$ ), where  $n_k \in F_{in}(n_i) \cup \{n_i\}$  and  $n_l \in F_{out}(n_j) \cup \{n_j\}$ . We first consider the feasibility condition of the top (bottom, left, or right) module if a reduction edge in  $C_h$  is moved to  $C_v$  as follows: Since the Move

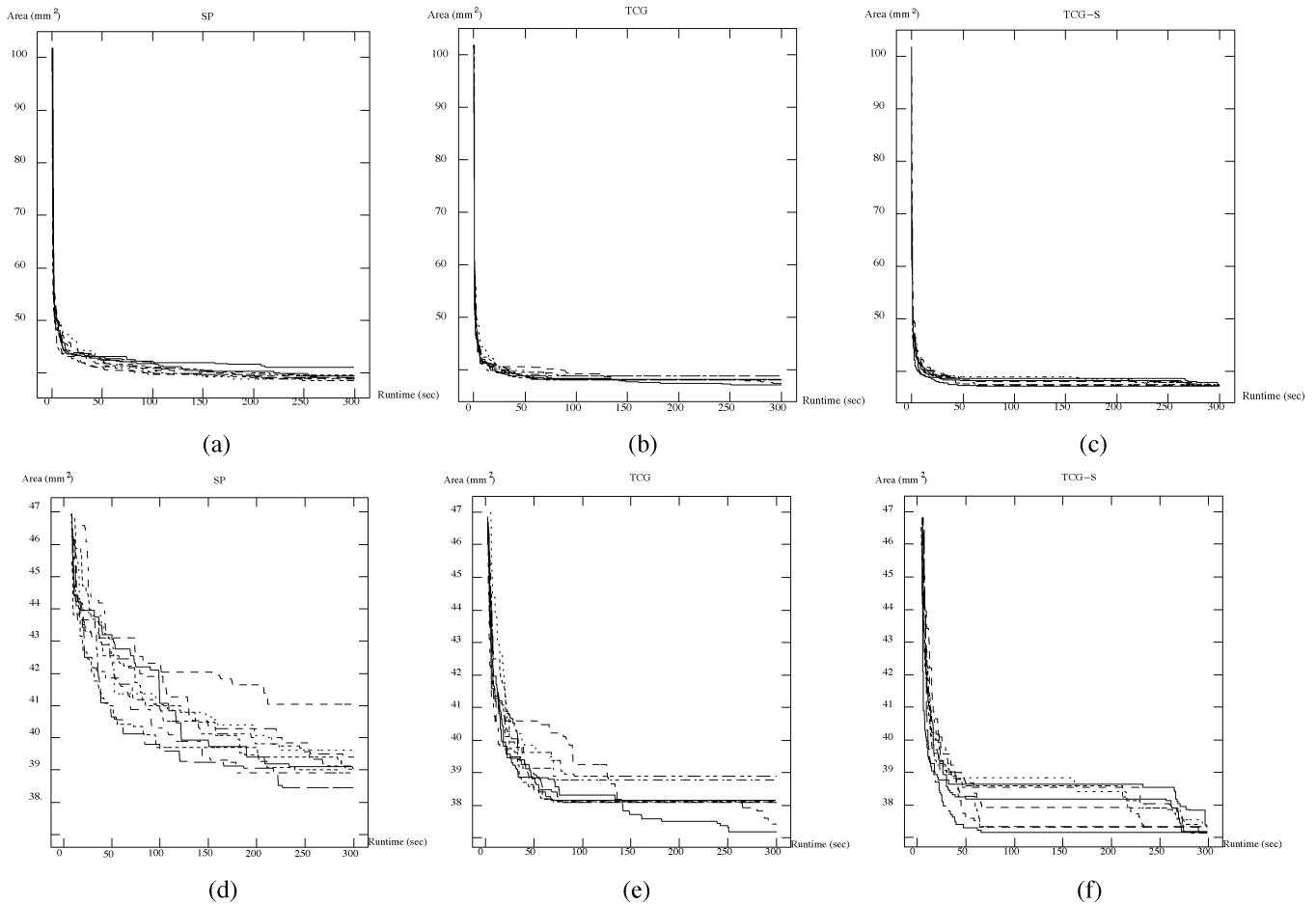


Fig. 9. Comparison for stability and convergence between SP, TCG, and TCG-S for ami49.

operation does not add any edge to  $C_v$  after an edge  $(n_i, n_j)$  in  $C_v$  is moved to  $C_h$ , it will not generate any new edge in the fanin (fanout) of a bottom (top) module in  $C_v$ . Therefore, the feasibility condition of the top (bottom) module is not violated. For a left boundary module  $b_q$ , suppose there exists an edge  $(n_p, n_q)$  in  $C_h$  after the operation.  $n_q$  is either  $n_j$  or a fanout of  $n_j$ . However, we do not move the edge  $(n_i, n_j)$  from  $C_v$  to  $C_h$  if  $n_j$  is a left boundary module. Besides,  $n_q$  cannot be a fanout of others in the original graph  $C_h$  if  $b_q$  is a left boundary module. Similarly, for the right boundary module  $b_p$ , suppose there exists an edge  $(n_p, n_q)$  in  $C_h$  after the edge  $(n_i, n_j)$  is moved to  $C_h$ .  $n_p$  is either  $n_i$  or a fanin of  $n_i$ . However, we do not move an edge  $(n_i, n_j)$  from  $C_v$  to  $C_h$  if  $n_i$  is a right boundary module. Besides,  $n_p$  cannot be a fanin of others in the original graph  $C_h$  if  $b_q$  is a right boundary module. Similar claims hold when an edge  $(n_i, n_j)$  is moved from  $C_v$  to  $C_h$ . ■

### B. TCG-S With Preplaced Modules

The placement with preplaced modules is to place a set of pre-specified modules at the designated locations of a chip, which can be formulated as follows:

**Definition 2: Preplaced Constraint:** Given a module  $b_i$  with a fixed coordinate  $(x_i, y_i)$  and an orientation,  $b_i$  must be placed at the designated location with the same orientation in the final packing.

Whether a preplaced module is packed at a correct location is not known until packing. Also, changing the coordinate of a module  $b_i$

may affect the packing for other modules after  $b_i$  in  $\Gamma_-$ . Therefore, we may need to modify a TCG-S to guarantee a feasible placement with the preplaced constraint after each perturbation.

Given a TCG-S, modules are packed one by one based on the sequence of  $\Gamma_-$ . A module  $b_i$  interacts with another module  $b_j$  if: 1)  $b_i$  overlaps  $b_j$ ; 2)  $b_j \vdash b_i$  and their projections on the  $y$  axis overlap; or 3)  $b_j \perp b_i$  and their projections on the  $x$  axis overlap. If  $b_i$  interacts with a preplaced module  $b_j$  and  $b_i$  was placed,  $n_i$  and  $n_j$  are swapped in the TCG-S to make  $b_j$  placed at the designated location. If a preplaced module  $b_i$  was placed and the resulting placement of  $b_i$  does not interact with itself at the designated location, we swap  $b_i$  with the node  $b_j$  right after  $b_i$  in  $\Gamma_-$ ; otherwise,  $b_i$  is placed at the designated location if there exists no module behind  $b_i$  in  $\Gamma_-$ .

Fig. 6(a) shows the resulting placement of the TCG-S of Fig. 2(g) without considering preplaced modules. Here, the heavily shaded rectangles, labeled  $D$  and  $E$ , give the correct locations for the preplaced modules  $b_d$  and  $b_e$ , respectively. As shown in the figure, the correct location for  $b_e$  ( $b_d$ ) is occupied by  $b_b$  ( $b_g$ ). Fig. 6(b)–(h) illustrate the process to transform an infeasible TCG-S into a feasible one with preplaced constraints. Fig. 6(b) and (c) show the placements after  $b_a$  and  $b_b$  are placed, respectively. Since  $b_b$  overlaps the region for the preplaced module  $b_e$  [see Fig. 6(c)], we swap  $b_b$  and  $b_e$  in TCG-S, and then place  $b_e$  at the designated location. (Note that  $b_b$  and  $b_e$  are exchanged in  $\Gamma_-$ .) Fig. 6(d) and (e) show the respective placements after  $b_c$  and the preplaced module  $b_d$  are placed. Since the preplaced module  $b_d$  does not intersect with itself at the designated coordinate [see Fig. 6(e)], we swap  $b_d$  and its successor  $b_b$  in  $\Gamma_-$ . (Note that  $b_d$  and  $b_b$  in  $\Gamma_-$  are exchanged.) Similarly, we swap  $b_d$  and  $b_g$  in TCG-S, resulting in the

TABLE IV  
AREA AND RUNTIME COMPARISONS BETWEEN [7] (ON PENTIUM-II 350) AND TCG-S (ON SUN SPARC ULTRA60) FOR PLACEMENT WITH BOUNDARY MODULES

Circuit	# T , # B , # L , # R	Lai et al. [7]		TCG-S	
		Area (mm <sup>2</sup> )	Time (sec)	Area (mm <sup>2</sup> )	Time (sec)
apte	1, 1, 1, 1	46.92	15	46.92	3
xerox	1, 1, 1, 1	20.4	19	19.977	33
hp	1, 1, 1, 1	9.24	23	9.158	26
ami33	2, 2, 2, 2	1.21	290	1.190	238
ami49	3, 3, 2, 3	36.84	601	36.765	584

placement shown in Fig. 6(f). Then,  $b_d$  is placed at the designated location in Fig. 6(g). Finally, the resulting placement after packing  $b_f$  is shown in Fig. 6(h).

## VII. EXPERIMENTAL RESULTS

Based on a simulated annealing method [6], we implemented the TCG-S representation in the C++ programming language on a 433-MHz SUN Sparc Ultra-60 workstation with 1 GB of memory. The code is available at <http://cc.ee.ntu.edu.tw/~ywchang/research.html>. Based on the five commonly used MCNC benchmark circuits listed in Table I, we conducted four experiments: 1) area optimization; 2) wirelength optimization; 3) solution convergence speed and stability; and 4) placement with boundary constraints. In Table I, Columns 2–5 list the respective numbers of modules, I/O pads, nets, and pins of the five circuits.

For Experiment 1, the area and runtime comparisons among SP, O-tree, B\*-tree, enhanced O-tree, CBL, and TCG are listed in Table II. As shown in Table II, TCG-S achieves best area utilization for the benchmark circuits in very efficient running times. Fig. 7 shows the resulting placement for ami49 with area optimization.

For Experiment 2, we estimated the wirelength of a net by half the perimeter of the minimum bounding box enclosing the net. The wirelength of a placement is given by the summation of the wirelengths of all nets. As shown in the Table III, TCG-S achieves the best average results in wirelength than O-tree, enhanced O-tree, and TCG using smaller running times. (Note that we did not compare with B\*-tree and CBL here since they did not report the results on optimizing wirelength alone.) Fig. 8 shows the resulting placement for ami49 with wirelength optimization.

In addition to the area and timing optimization, in Experiment 3, we also compared the solution convergence speed and stability among SP, TCG, and TCG-S to eliminate the possible unfairness due to the non-deterministic behavior of simulated annealing, which were neglected in most previous works. (Note that other tools are not available to us for the comparative study.) We randomly ran SP, TCG, and TCG-S on ami49 ten times based on the same initial placement whose area is 102 mm<sup>2</sup>. The resulting areas are plotted as functions of the running times (sec). Figs. 9(a)–(c) show the resulting curves of SP, TCG, and TCG-S, respectively. To see the detailed convergence rates, we show in Figs. 9 only the portions whose areas are smaller than 47 mm<sup>2</sup>. As illustrated in Fig. 9(c), TCG-S converges very fast to desired solutions, and the results are very stable ( $\leq 37.5$  mm<sup>2</sup> for all runs). In contrast, the convergence speed of SP is much slower than TCG-S and TCG, and the resulting areas are often larger than 39 mm<sup>2</sup>. Further, there is a large variance in its final solutions. Based on the experimental results, we rank the convergence speed from the fastest to the slowest and the solution stability from the most stable to the least stable as follows: TCG – S  $\succ$  TCG  $\succ$  SP. We note that the stability and convergence speed should be very important metrics to evaluate the quality

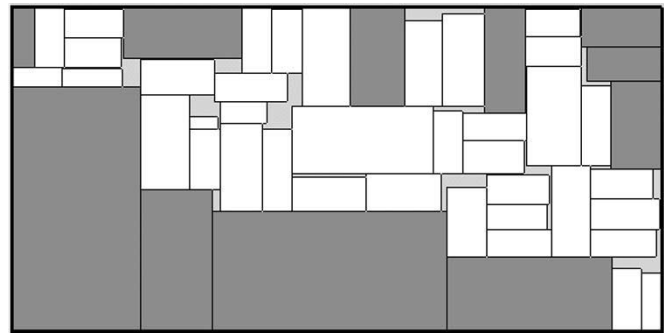


Fig. 10. Resulting placement of ami49 with boundary modules being heavily shaded ( $(\#|T|, \#|B|, \#|L|, \#|R|) = (3, 3, 2, 3)$ , area = 36.765 mm<sup>2</sup>). Note that the lightly shaded regions denote dead spaces.

of a floorplan representation because they reveal the corresponding solution structure for optimization. However, they were often ignored in previous works. (Most previous works focus on the comparison of solution space and packing complexity. Nevertheless, we find that the solution structure induced by a representation plays an even more important role in floorplan optimization.)

For the experiments with boundary modules, we compared TCG-S with the SP-based method in [7] using the same data generated by [7]. The second column of Table IV shows the numbers of the top, bottom, left, and right modules, denoted by  $\#|T|$ ,  $\#|B|$ ,  $\#|L|$ , and  $\#|R|$ , respectively. As shown in Table IV, TCG-S obtains smaller silicon areas than [7]. Fig. 10 shows the resulting placement for ami49 with boundary modules.

## VIII. CONCLUDING REMARKS

We have presented the TCG-S representation for general floorplans by combining the advantages of two most promising P\*-admissible representations TCG and SP and, at the same time, eliminating their disadvantages. We also have proposed a loglinear-time packing scheme for a P\*-admissible representation. We note that this scheme can also be applied to most existing representations, such as SP and BSG. Based on our theoretical study and extensive experiments, we also have shown the superior capability, efficiency, stability, and flexibility of TCG-S for floorplan design.

## ACKNOWLEDGMENT

The authors would like to thank the anonymous reviewers for their very constructive comments.

## REFERENCES

- [1] Y. C. Chang, Y. W. Chang, G. M. Wu, and S. W. Wu, "B\*-trees: A new representation for nonslicing floorplans," in *Proc. Design Automation Conf.*, 2000, pp. 458–463.
- [2] T. Cormen, C. Leiserson, R. Rivest, and C. Stein, *Introduction to Algorithms*, 2nd ed. New York: MIT Press/McGraw-Hill, 2001.
- [3] P.-N. Guo, C.-K. Cheng, and T. Yoshimura, "An O-tree representation of nonslicing floorplan and its applications," in *Proc. Design Automation Conf.*, 1999, pp. 268–273.
- [4] X. Hong, G. Huang, T. Cai, J. Gu, S. Dong, C.-K. Cheng, and J. Gu, "Corner block list: An effective and efficient topological representation of nonslicing floorplan," in *Proc. Int. Conf. Computer-Aided Design*, 2000, pp. 8–12.
- [5] Y. Hu, J. Lai, and T.-C. Wang, "A complete set of operations for perturbing transitive closure graphs," 2003, submitted for publication.
- [6] S. Kirkpatrick, C. D. Gelatt, and M. P. Vecchi, "Optimization by simulated annealing," *Science*, vol. 220, no. 4598, pp. 671–680, May 1983.

- [7] J.-B. Lai, M.-S. Lin, T.-C. Wang, and L.-C. Wang, "Module placement with boundary constraints using the sequence-pair," in *Proc. Asia South Pacific-Design Automation Conf.*, 2001, pp. 515–520.
- [8] E. Lawler, *Combinatorial Optimization: Networks and Matroids*. New York: Holt, Rinehart, and Winston, 1976.
- [9] J.-M. Lin and Y.-W. Chang, "TCG: A transitive closure graph-based representation for nonslicing floorplans," in *Proc. Design Automation Conf.*, 2001, pp. 764–769.
- [10] —, "TCG-S: Orthogonal coupling of  $P^*$ -admissible representations for general floorplans," in *Proc. Design Automation Conf.*, 2002, pp. 842–847.
- [11] —, "TCG: A transitive closure graph-based representation for general floorplans," *IEEE Trans. VLSI Syst.*, 2003.
- [12] Y. Ma, S. Dong, X. Hong, Y. Cai, C. K. Cheng, and J. Gu, "VLSI floorplanning with boundary constraints based on corner block list," in *Proc. Asia South Pacific-Design Automation Conf.*, 2001, pp. 509–514.
- [13] H. Murata, K. Fujiyoshi, S. Nakatake, and Y. Kajitani, "Rectangle-packing based module placement," in *Proc. Int. Conf. Computer-Aided Design*, 1995, pp. 472–479.
- [14] H. Murata, K. Fujiyoshi, and M. Kaneko, "VLSI/PCB placement with obstacles based on sequence pair," in *Proc. Int. Symp. Phys. Design*, 1997, pp. 26–31.
- [15] S. Nakatake, K. Fujiyoshi, H. Murata, and Y. Kajitani, "Module placement on BSG-structure and IC layout applications," in *Proc. Int. Conf. Computer-Aided Design*, 1996, pp. 484–491.
- [16] R. H. J. M. Otten, "Automatic floorplan design," in *Proc. Design Automation Conf.*, 1982, pp. 261–267.
- [17] Y. Pang, C. K. Cheng, and T. Yoshimura, "An enhanced perturbing algorithm for floorplan design using the O-tree representation," in *Proc. Int. Symp. Phys. Design*, 2000, pp. 168–173.
- [18] X. Tang and D. F. Wong, "FAST-SP: A fast algorithm for block placement based on sequence pair," in *Proc. Asia South Pacific-Design Automation Conf.*, 2001, pp. 521–526.
- [19] D. F. Wong and C. L. Liu, "A new algorithm for floorplan design," in *Proc. Design Automation Conf.*, 1986, pp. 101–107.

## A Unified Framework for Generating All Propagation Functions for Logic Errors and Events

Maria K. Michael, Themistoklis Haniotakis, and Spyros Tragoudas

**Abstract**—We present a generic framework that supports efficient generation of the traditional Boolean difference function of some output with respect to any line in a combinational circuit, which is important when testing for logic defects. The framework also allows for the generation of generalized Boolean difference functions, which reflect sensitivity on event propagation from a given line to some circuit output. This generalized function could apply in timing verification, analysis, and test. We implemented the proposed framework using various function representation environments, including binary decision diagrams, Boolean expression diagrams, and Boolean networks, and report experimental results on the ISCAS'85 and ISCAS'89 benchmarks.

**Index Terms**—Automatic test pattern generation (ATPG), delay testing, testing, timing analysis, verification.

### I. INTRODUCTION

The problem of generating the propagation functions of all lines in a combinational (or fully scanned sequential) circuit is examined. The propagation function of a circuit line is a Boolean function that represents all the possible primary input assignments that allow for a change on the line to be observed (propagated) at some primary output.

Let  $a$  be any circuit line and  $z$  a primary output. For simplicity, we use the above symbols to also denote the functionality of the respective lines. The propagation function indicating whether line  $z$  is sensitive to logic changes on line  $a$  is also known as the *Boolean difference of function  $z$  with respect to function  $a$* , and is defined as  $(\partial z / \partial a)$ .

Function-based automatic test pattern generation (ATPG) methods typically use the Boolean Difference function as their basis ([4], [12]) because it indicates whether an activated *logic error* propagates from line  $a$  to output  $z$ .<sup>1</sup> For this reason, the Boolean difference function is also called the *logic-error propagation function of  $z$  with respect to  $a$* . Although function-based ATPG methods are slower than structural-based ATPG methods, they increasingly gain popularity due to advances in data structures that store and manipulate functions. These include binary decision diagrams (BDDs) [2], that are canonical forms, and noncanonical forms, such as Boolean networks (BNETS) [1], Boolean expression diagrams (BEDs) [7], conjunctive normal forms, among others. In addition, function-based methods inherently allow for such implicit representations of many test patterns per fault (in the case where BDDs are used, all test patterns per fault are represented) that can be easily manipulated using basic Boolean concepts to help in other test-related problems such as test set compaction ([6], [8]) and on-chip test-set embedding. Moreover, function-based methods can speed up the detection of those faults that are hard to detect by the structural methods. It is noted that function-based ATPG approaches as in [3], [5], [9], [14], and [15], among others, do not create distinct functions for fault activation and fault propagation in

Manuscript received October 9, 2002; revised June 18, 2003 and August 19, 2003. This paper was recommended by Associate Editor S. M. Reddy.

M. K. Michael is with the Electrical and Computer Engineering Department, University of Cyprus, CY-1678 Nicosia, Cyprus (e-mail: mmichael@ucy.ac.cy).

T. Haniotakis and S. Tragoudas are with the Electrical and Computer Engineering Department, Southern Illinois University, Carbondale, IL 62901 USA (e-mail: haniotak@siu.edu; spyros@enr.siu.edu).

Digital Object Identifier 10.1109/TCAD.2004.828112

<sup>1</sup>Logic error is understood as a fault (in the ATPG context) or a design error (in the verification context).